THE JOURNAL OF PHYSICAL CHEMISTRY B

Article

pubs.acs.org/JPCB

Generic Schemes for Single-Molecule Kinetics. 2: Information Content of the Poisson Indicator

Thomas R. Avila,[†,‡] D. Evan Piephoff,[†,‡] and Jianshu Cao*[,†]

[†]Department of Chemistry, Massachusetts Institute of Technology, Cambridge, Massachusetts 02139, United States

ABSTRACT: Recently, we described a pathway analysis technique (paper 1) for analyzing generic schemes for single-molecule kinetics based upon the first-passage time distribution. Here, we employ this method to derive expressions for the Poisson indicator, a normalized measure of stochastic variation (essentially equivalent to the Fano factor and Mandel's Q parameter), for various renewal (i.e., memoryless) enzymatic reactions. We examine its dependence on substrate concentration, without assuming all steps follow Poissonian kinetics. Based upon fitting to the functional forms of the first two waiting time moments, we show that, to second order, the non-Poissonian kinetics are generally underdetermined but can be specified in certain scenarios. For an enzymatic reaction with an arbitrary intermediate topology, we identify a generic minimum of the Poisson indicator as a function of substrate concentration, which can be used to tune substrate concentration to the stochastic fluctuations and to estimate the largest number of underlying consecutive links in a turnover cycle. We identify a local maximum of the Poisson indicator (with respect to substrate concentration) for a renewal process as a signature of competitive binding, either between a substrate and an inhibitor or between multiple substrates. Our analysis explores the rich connections between Poisson indicator measurements and microscopic kinetic mechanisms.

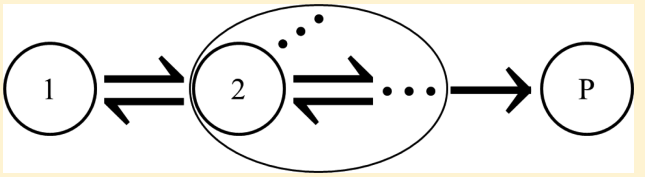

1. INTRODUCTION

Single-molecule spectroscopy techniques have allowed the study of single biomolecular complexes at a level of detail previously unattainable.[1] Escaping the averaging of measured quantities inherent in ensemble measurements, single-molecule studies offer insights into the details of the dynamic behavior of biomolecules.[2,3] In particular, these studies provide information on the underlying kinetic scheme that is unavailable through traditional, bulk measurements of chemical kinetics.[4,5] At their core, single-molecule studies of enzymes and motor proteins interrogate the waiting time between reaction events, such as the conversion of substrate to product or the stepping of a motor protein along a filament. The waiting time varies stochastically over the course of the observation of the molecule, and sufficiently long time traces allow the waiting time probability distribution to be described.[6] Given a kinetic mechanism, a mathematical expression for this waiting time distribution in terms of kinetic parameters, such as rate constants and reactant or product concentrations, may be derived. Furthermore, expressions for the moments of the distribution and the correlations between events may be obtained and compared to experimental observations.

From a theoretical standpoint, it is important to first determine the information content available from single-molecule data[7] and then make connections to a generic scheme. Previous work has addressed the relation of single-molecule data to reaction network connectivity and developed a mathematical framework for treating data within a given reaction scheme.[6,8−14] In a complementary fashion, we have described a pathway analysis approach to generic reaction schemes for single-molecule kinetics (paper 1).[15] In contrast to other approaches, pathway analysis may be easily adapted to arbitrary reaction scheme topologies. This method provides a straightforward prescription for decomposing a proposed scheme via two basic kinetic motifs, sequential and branching. Second, our approach requires no assumption of Poissonian kinetics (i.e., rate processes), allowing each step to be treated with the greatest possible generality. As in paper 1,[15] the current study deals with renewal (i.e., memoryless) processes and, as a result, does not capture memory effects in the action of single enzymes, as described previously experimentally and theoretically.[6,16] A subsequent paper will generalize our method to arbitrary nonrenewal processes (paper 3).

This previous work[15] provided calculation of the first waiting time moment (i.e., mean first-passage time) for generalized enzymatic schemes, which is directly related to the turnover rate for the process. The turnover rate and mean first-passage time can be determined from ensemble-averaging; however, higher-order moments, which contain information on the underlying kinetic scheme of the enzymatic reaction,[17−21] are unique to single-molecule measurements. In particular, the Poisson indicator, a measure of stochastic fluctuations,[15] captures deviation from Poissonian statistics, taking on a positive value for bunching behavior, a negative value for antibunching behavior, and vanishing for a Poisson process.[22] The dependence of the Poisson indicator on substrate concentration can then inform which steps adhere to or violate Poissonian statistics. Moreover, the Poisson indicator is

Received: February 15, 2017
Revised: June 8, 2017
Published: June 14, 2017

DOI: 10.1021/acs.jpcb.7b01516
J. Phys. Chem. B XXXX, XXX, XXX−XXX

essentially equivalent to other normalized measures of the variance, including Mandel's Q parameter from photon statistics,[23] the randomness parameter from studies of molecular motors,[24] and the Fano factor.[25]

This paper is organized as follows: in section 2, we extend the previously introduced pathway analysis to the calculation of the second moment of the waiting time distribution. We examine a generic model of enzymatic reactions that can generate all possible kinetic models with the same basic topological connectivity and contains no assumptions upon the form of the underlying kinetic scheme. As stated earlier, the only constraint is that the overall reaction must be a renewal process. In section 3.1, we employ this approach for the generic enzymatic reaction to evaluate the maximal information content of experimental determinations of the second waiting time moment and, in particular, to examine the dependence of the second moment on substrate concentration. Our results include functional forms for the dependence of both the first (related to the turnover rate) and second (related to the Poisson indicator) reaction waiting time moments on substrate concentration, as well as explicit expressions in terms of the waiting time moments for individual steps. We analyze these functional forms and explore their connections to important experimental limits. In sections 3.2 and 3.3, we extend earlier, similar results[19,20] to the more complex cases of competitive inhibition and competition between multiple substrates, respectively, and the resulting expressions for the Poisson indicator differ qualitatively from these earlier results. In section 4, we conclude.

2. THEORETICAL METHODS

Let $\phi(t)$ represent the waiting time distribution, which describes the distribution of times between successive reaction events. The moments of the waiting time distribution are given by $\langle t^n \rangle = \int_0^\infty t^n \phi(t) \mathrm{d}t = (-1)^n \frac{\mathrm{d}^n \hat{\phi}(s)}{\mathrm{d}s^n}\Big|_{s=0}$, where $\hat{\phi}(s)$ denotes the Laplace transform of $\phi(t)$, defined as $\hat{\phi}(s) = \int_0^\infty e^{-st}\phi(t)\,\mathrm{d}t$. Our challenge is then to formulate the waiting time distribution for a generic enzymatic reaction. The model we treat is illustrated in Figure 1. Here, states 1 and 2 are connected by a reversible step, with an arbitrary topology after state 2, before a final, irreversible transition (or set of transitions)—which can be experimentally monitored—to product P. Upon the creation of a product molecule, we assume that the enzyme regenerates quickly and irreversibly to state 1 (the initial free enzyme state), where it begins another turnover. In our model, enzyme turnover is a renewal process because it always begins in the same state. In keeping with the Michaelis–Menten model of enzymatic reactions, the first step corresponds to substrate binding to the enzyme,[15] which we assume to have a single substrate-binding site, making this the only step with dependence on substrate concentration. There may exist many intermediate underlying states between the substrate binding step and final transition(s) to product. We refer to this (possible) aggregate of states as the bound/intermediate state B, which may undergo non-Poissonian decay due to its (possible) internal dynamics, some of which may involve branching out of the chain as well as cyclic loops.

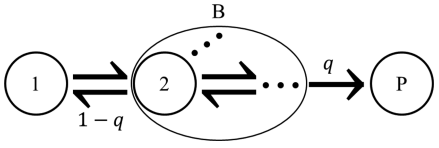

Figure 1. Generic enzymatic reaction scheme. The aggregate of intermediate states between the initial free enzyme (state 1) and final transition(s) to product P, referred to as the bound/intermediate state B, has an arbitrary internal topology. q denotes the branching probability for advancing to product from state 2.

Now, if we let $Q_{ij}(s)$ denote the waiting time distribution for the i-to-j transition in the Laplace domain, we can write the overall waiting time (i.e., first-passage time) distribution in the Laplace domain as

$$\hat{\phi}(s) = \frac{Q_{1P}(s)}{1 - \tilde{Q}_{11}(s)} = Q_{1P}(s)[1 + \tilde{Q}_{11}(s) + \tilde{Q}_{11}(s)^2 + \tilde{Q}_{11}(s)^3 + ...] \quad (1)$$

where $Q_{1P}(s)$ is the waiting time distribution for the passage from state 1 to the product, and $\tilde{Q}_{11}(s)$ represents the waiting time distribution for the passage out of and back to state 1.[15] Each term in the infinite summation can be understood as follows: the first term corresponds to the passage from state 1 to product P without returning to state 1, the second term corresponds to the passage from state 1 to product P while returning to state 1 exactly once, the third term corresponds to the passage while returning to state 1 exactly twice, and so on and so forth. Examining only the initial free enzyme state and the bound/intermediate state, we can write

$$Q_{1P}(s) = Q_{1B}(s)Q_{BP}(s) \quad (2)$$

$$\tilde{Q}_{11}(s) = Q_{1B}(s)Q_{B1}(s) \quad (3)$$

where $Q_{1B}(s)$ is the waiting time distribution for substrate binding, $Q_{B1}(s)$ is the waiting time distribution for substrate unbinding, and $Q_{BP}(s)$ is the waiting time distribution for product formation (i.e., the conversion of substrate to product after binding). Now, the overall waiting time distribution is given by

$$\hat{\phi}(s) = \frac{Q_{1B}(s)Q_{BP}(s)}{1 - Q_{1B}(s)Q_{B1}(s)} \quad (4)$$

This scheme comprises a generic model for enzyme kinetics. It treats explicitly the substrate binding step with waiting time distribution $Q_{1B}(s)$, while treating in generality the decay of the bound/intermediate state with the distributions $Q_{B1}(s)$ and $Q_{BP}(s)$.

In the Laplace domain, these waiting time distributions can be expanded in terms of their moments as

$$Q_{ij}(s) = q_{ij}\left(1 - s\langle t_{ij}\rangle + \frac{s^2}{2}\langle t_{ij}^2\rangle - \cdots\right) \quad (5)$$

where the branching probabilities q_{ij} account for the normalization of probability, with $\sum_j q_{ij} = 1$ and $\sum_j q_{ij}\langle t_{ij}^k\rangle = \langle \tau_i^k\rangle$, the k^{th} moment for the decay time (i.e., dwell time) of state i. Expanding the overall waiting time distribution in terms of the moments for the individual steps, as in eq 5, yields

$$\hat{\phi}(s) = \frac{\alpha}{1 - \beta} \quad (6)$$

with

DOI: 10.1021/acs.jpcb.7b01516
J. Phys. Chem. B XXXX, XXX, XXX−XXX

$$\alpha = q\left[1 - s\langle\tau_1 + t_{BP}\rangle + \frac{s^2}{2}\langle(\tau_1 + t_{BP})^2\rangle - \ldots\right] \quad (7)$$

$$\beta = (1 - q)\left[1 - s\langle\tau_1 + t_{B1}\rangle + \frac{s^2}{2}\langle(\tau_1 + t_{B1})^2\rangle - \ldots\right] \quad (8)$$

where $\langle\tau_1\rangle$ and $\langle\tau_1^2\rangle$ are the first and second waiting time moments for the decay of the initial free enzyme state, $\langle t_{BP}\rangle$ and $\langle t_{BP}^2\rangle$ are the first and second waiting time moments for product formation, and $\langle t_{B1}\rangle$ and $\langle t_{B1}^2\rangle$ are the first and second moments for substrate unbinding. The product formation branching probability q expresses the probability of advancing to product after substrate binding. From an expression for the overall waiting time distribution, the calculation of waiting time moments is straightforward. Given $\hat{\phi}(s) = \frac{\alpha}{1-\beta}$, and observing that $(1 - \beta)\,|_{s=0} = \alpha|_{s=0}$, the first moment (i.e., mean first-passage time) is expressed as

$$\langle t\rangle = -\frac{d\hat{\phi}(s)}{ds}\bigg|_{s=0} = \frac{-(\dot{\alpha} + \dot{\beta})}{\alpha}\bigg|_{s=0} \quad (9)$$

where $\dot{x}$ denotes differentiation of x with respect to the Laplace variable.

While the mean first-passage time can be determined from bulk measurements, higher-order moments, which contain information on microscopic mechanisms,[17−21,26] are unique to single-molecule analysis. The Poisson indicator, which measures stochastic fluctuations, is expressed as[15] $Q(t) = \frac{\langle N(t)^2\rangle - \langle N(t)\rangle^2}{\langle N(t)\rangle} - 1$, where $\langle N(t)\rangle$ and $\langle N(t)^2\rangle$ are the first and second moments for the number of turnover events N occurring within the measurement time window t. The first moment $\langle N(t)\rangle$ is asymptotically related to the mean first-passage time as[22] $\langle N(t)\rangle \sim t/\langle t\rangle$. We are interested in the long-time limit $P \equiv \lim_{t\to\infty} Q(t)$, which we simply refer to hereafter as the Poisson indicator (essentially equivalent to the Fano factor[25] and Mandel's Q parameter[23]). Asymptotically, $N(t)$ is Gaussian distributed for a renewal process, with[27] $\langle N(t)^2\rangle - \langle N(t)\rangle^2 \sim \frac{\langle t^2\rangle - \langle t\rangle^2}{\langle t\rangle^3} t$, resulting in[22]

$$P = \frac{\langle t^2\rangle - 2\langle t\rangle^2}{\langle t\rangle^2} \quad (10)$$

The Poisson indicator describes the deviation of a statistical process from Poissonian behavior, assuming a positive value for the bunching of events (super-Poissonian statistics), a negative value for the antibunching of events (sub-Poissonian statistics), and vanishing for a Poisson process.[22] This quantity and equivalent measures of variation are frequently calculated in experimental studies and can serve to indicate the presence of dynamic disorder in particular reaction steps.[17] Of particular interest, the sign of the Poisson indicator yields information about the topology of the kinetic mechanism: negative values of P correspond to kinetics dominated by sequential, multistep reactions, while positive values of P are associated with kinetics dominated by a competing trapping process.[20,28] In fact, when no branching occurs out of an enzymatic chain with an irreversible final step, $P \leq 0$.[28] Given the above functional form for $\hat{\phi}(s)$, the numerator of the Poisson indicator can be calculated as

$$\langle t^2\rangle - 2\langle t\rangle^2 = \frac{\ddot{\alpha} + \ddot{\beta}}{\alpha} - \frac{2\dot{\alpha}}{\alpha^2}(\dot{\alpha} + \dot{\beta})\bigg|_{s=0} \quad (11)$$

3. RESULTS AND DISCUSSION

3.1. Generic Enzymatic Reaction. Applying eqs 6−9 and 11 to the generic model of enzyme catalysis (Figure 1) yields

$$\langle t\rangle = \frac{1}{q}[\langle\tau_1\rangle + \langle\tau_B\rangle] \quad (12)$$

$$\langle t^2\rangle - 2\langle t\rangle^2 = \frac{1}{q}[\langle\tau_1^2\rangle - 2\langle\tau_1\rangle^2 + \langle\tau_B^2\rangle - 2\langle t_{BP}\rangle(\langle\tau_1\rangle + \langle\tau_B\rangle)] \quad (13)$$

where $\langle\tau_B\rangle = q\langle t_{BP}\rangle + (1 - q)\langle t_{B1}\rangle$ and $\langle\tau_B^2\rangle = q\langle t_{BP}^2\rangle + (1 - q)\langle t_{B1}^2\rangle$ are the first and second waiting time moments, respectively, for bound/intermediate state decay.

3.1.1. Functional Forms and Parameter Specification. In order to connect the above expressions to experimental determinations of the Poisson indicator, we must examine their dependence on substrate concentration [S]. This dependence can be addressed by treating substrate binding as a pseudo-first-order rate step, which implies that substrate binding is a Poisson process (i.e., $\langle\tau_1^2\rangle - 2\langle\tau_1\rangle^2 = 0$) and $\langle\tau_1\rangle = \frac{1}{k_{1B}}$, with pseudo-first-order rate $k_{1B} = k_{1B}^\circ[S]$, where k_{1B}° is the rate constant for substrate binding. Experimental studies of single enzymes have confirmed the validity of this assumption,[16] and its application leads to

$$\langle t\rangle = \frac{1}{q}\left[\frac{1}{k_{1B}^\circ[S]} + \langle\tau_B\rangle\right] \quad (14)$$

$$\langle t^2\rangle - 2\langle t\rangle^2 = \frac{1}{q}\left[\frac{-2\langle t_{BP}\rangle}{k_{1B}^\circ[S]} + \langle\tau_B^2\rangle - 2\langle\tau_B\rangle\langle t_{BP}\rangle\right] \quad (15)$$

Finally, the Poisson indicator for the enzymatic reaction is given by

$$P([S]) = \frac{q\left[\frac{-2k_{1B}^\circ\langle t_{BP}\rangle}{[S]} + (k_{1B}^\circ)^2(\langle\tau_B^2\rangle - 2\langle\tau_B\rangle\langle t_{BP}\rangle)\right]}{\left(\frac{1}{[S]} + k_{1B}^\circ\langle\tau_B\rangle\right)^2} \quad (16)$$

This result gives a general functional form for the substrate dependence of the Poisson indicator under the assumption of pseudo-first-order kinetics for substrate binding:

$$P([S]) = \frac{\frac{A}{[S]} + B}{\left(\frac{1}{[S]} + C\right)^2} \quad (17)$$

for constants A, B, and C independent of [S], with expressions

$$A = -2qk_{1B}^\circ\langle t_{BP}\rangle \quad (18)$$

$$B = q(k_{1B}^\circ)^2(\langle\tau_B^2\rangle - 2\langle\tau_B\rangle\langle t_{BP}\rangle) \quad (19)$$

$$C = k_{1B}^\circ\langle\tau_B\rangle \quad (20)$$

This result is analogous to those reported elsewhere.[19,20,29]

From eqs 14 and 16, we see that, to second order, five parameters are needed to describe the non-Poissonian kinetics

DOI: 10.1021/acs.jpcb.7b01516
J. Phys. Chem. B XXXX, XXX, XXX−XXX

of the generic enzymatic reaction (with Poissonian binding): k°_{1B}, q, $\langle\tau_B\rangle$, $\langle t_{BP}\rangle$, and $\langle\tau_B^2\rangle$. However, fitting measured data to these functional forms (with respect to [S]) for the first waiting time moment and Poisson indicator together only gives four independent parameters, $[qk^{\circ}_{1B}]^{-1}$, $\langle\tau_B\rangle/q$, A, and B, since C (given in eq 20) is not independent of $[qk^{\circ}_{1B}]^{-1}$ and $\langle\tau_B\rangle/q$. Thus, to second order, the generic scheme kinetics are underdetermined by one parameter. However, if k°_{1B} is known or can be estimated, then the kinetics can be specified. Alternatively, if the enzyme is highly efficient (referred to as a "perfectly evolved enzyme"[30]), such that the turnover rate is limited only by the rate of diffusion of substrate to the active site of the enzyme, we may assume that virtually every substrate binding event leads to product. In our model, this corresponds to $q \approx 1$, which results in $\langle\tau_B\rangle \approx \langle t_{BP}\rangle$ and $\langle\tau_B^2\rangle \approx \langle t_{BP}^2\rangle$. Now, three parameters are needed to describe the kinetics, and three can be obtained from fitting (since A is no longer independent of $[qk^{\circ}_{1B}]^{-1}$ and $\langle\tau_B\rangle/q$); thus, the kinetics can be specified under this assumption. Additionally, if the bound/intermediate state undergoes Poissonian decay (i.e., the unbinding and product formation transitions are rate steps), then $\langle\tau_B^2\rangle - 2\langle\tau_B\rangle^2 = 0$ and $\langle\tau_B\rangle = \langle t_{B1}\rangle = \langle t_{BP}\rangle$, eliminating two kinetic parameters and causing B (given in eq 19) to vanish, thereby permitting the kinetics to be specified. It should also be noted that our result for the first waiting time moment (eq 14) follows the Michaelis–Menten functional form; this is consistent with earlier work demonstrating that mechanisms of arbitrary complexity yield a turnover rate with a hyperbolic dependence on [S] for zero conformational current.[31−33] Representative plots of the Poisson indicator versus [S] appear in Figure 2. Qualitatively, the Poisson indicator approaches finite limits at small and large [S] and may feature a local minimum.

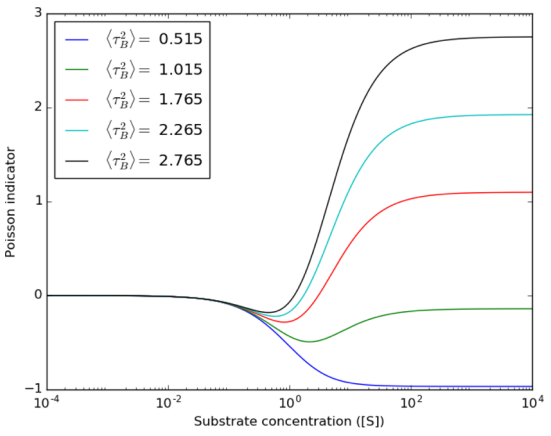

Figure 2. Plot of the Poisson indicator versus substrate concentration for the generic enzymatic reaction (eq 16). The kinetic parameters chosen are $k^{\circ}_{1B} = 1$, $q = 0.5$, $\langle\tau_B\rangle = 0.55$, and $\langle t_{BP}\rangle = 1$, with $\langle\tau_B^2\rangle$ given in the legend.

3.1.2. Minimum of Poisson Indicator and Topological Bound. The Poisson indicator is a measure of dispersion in $N(t)$, with sub-Poissonian statistics corresponding to less dispersion than that for a Poisson process. For nonzero A and C, when $B > 0$, $P([S]) < 0$ for $0 < [S] < -A/B$; when $B \leq 0$, $P([S]) < 0$ for $[S] > 0$. Thus, for any set of obtainable, nonzero A and C, there always exists a (finite or infinite) range of substrate concentrations at which sub-Poissonian behavior is achievable, even when branching occurs within the bound/intermediate state. The Poisson indicator as a function of [S] has one stationary point at

$$[S]^* = \left[k^{\circ}_{1B}\left(\frac{\langle\tau_B^2\rangle}{\langle t_{BP}\rangle} - \langle\tau_B\rangle\right)\right]^{-1} \tag{21}$$

which is only realizable when $[S]^* \geq 0$. For (i) $\langle\tau_B^2\rangle > \langle\tau_B\rangle\langle t_{BP}\rangle$, $P([S])$ is minimized at $[S]^*$, where $P([S]^*) = -q\langle t_{BP}\rangle^2/\langle\tau_B^2\rangle$, which can never correspond to a local maximum. For (ii) $\langle\tau_B^2\rangle \leq \langle\tau_B\rangle\langle t_{BP}\rangle$, $P([S])$ is monotonic and achieves a minimum of $q(\langle\tau_B^2\rangle - 2\langle\tau_B\rangle\langle t_{BP}\rangle)/\langle\tau_B\rangle^2$ as $[S] \to \infty$ ($\langle\tau_B^2\rangle = 0.515$ curve in Figure 2). In either case, the minimum of $P([S])$ corresponds to the point of minimal dispersion (with respect to [S]); thus, [S] can be tuned to the stochastic fluctuations to minimize turnover event dispersion.

For the reaction of an enzyme with a single binding site and an irreversible final step (or set of steps), the Poisson indicator is bounded by[34] $P \geq M_{max}^{-1} - 1$, where M_{max} is the largest value of M, the number of consecutive links in a turnover cycle, with a network possibly containing multiple turnover cycles. In our model, for a unicyclic network (which may still involve branching within the bound/intermediate state), M (and hence, M_{max}) corresponds to the number of underlying sequential (unbranched) rate steps in the scheme; however, since the bound/intermediate state can contain cyclic loops, and since multiple underlying transitions to product can be present, the generic scheme can represent a multicyclic network. The corresponding bound for M_{max} is given by $M_{max} \geq [P + 1]^{-1}$, which is saturated when all links in the turnover cycle that corresponds to M_{max} are irreversible with identical rates and the rates of any branching steps out of this cycle are zero, which corresponds to the longest homogeneous, sequential chain that can be formed in the network.[34] This topological bound can be modified using the minimum of $P([S])$. For (i) $\langle\tau_B^2\rangle > \langle\tau_B\rangle\langle t_{BP}\rangle$, M_{max} is bounded by

$$M_{max} \geq \left[1 - q\frac{\langle t_{BP}\rangle^2}{\langle\tau_B^2\rangle}\right]^{-1} \tag{22}$$

For (ii) $\langle\tau_B^2\rangle \leq \langle\tau_B\rangle\langle t_{BP}\rangle$, we have

$$M_{max} \geq \left[1 + q\frac{\langle\tau_B^2\rangle - 2\langle\tau_B\rangle\langle t_{BP}\rangle}{\langle\tau_B\rangle^2}\right]^{-1} \tag{23}$$

Thus, eq 22 or 23 can be used to estimate the largest number of underlying consecutive rate steps in a turnover cycle (see Appendix A for a demonstrative example). Notably, both of these bounds are independent of k°_{1B}, as are the inequalities identifying the two cases. We note that even though the generic scheme kinetics are generally underdetermined by one parameter, the expressions in eqs 21–23, along with the minimum of $P([S])$ (and $\langle\tau_B^2\rangle/(\langle\tau_B\rangle\langle t_{BP}\rangle)$ to identify the case), can be evaluated from measurements of the first two waiting time moments and [S], without the need for any assumptions.

3.1.3. Limiting Behavior of Poisson Indicator. The pathway analysis described above offers a simple route to the calculation of waiting time moments, without the assumption of a particular rate model. Ultimately, the goal is to connect experimental determinations of waiting time moments to features of the underlying mechanism. From the analytical expressions for the Poisson indicator as a function of substrate

DOI: 10.1021/acs.jpcb.7b01516
J. Phys. Chem. B XXXX, XXX, XXX−XXX

concentration, we can now examine the experimentally accessible limits.

As can be seen from eq 16, in the limit of low substrate concentration, the Poisson indicator vanishes. This is a consequence of the assumption that substrate binding is a pseudo-first-order rate process. At very low substrate concentration, substrate binding becomes the rate-determining step for the enzymatic process. Since the Poisson indicator reflects the statistical properties of the waiting time for the overall reaction, if the waiting time for the reaction is dominated by a single step, the Poisson indicator will reflect the statistical properties of that step. Hence, at very low substrate concentration, the Poisson indicator vanishes. This is supported by the experimental observation of Poissonian kinetics for single enzymes at very low substrate concentrations.[16] As is also apparent from eq 16, at low substrate concentration, we have, to leading order,

$$P([\mathrm{S}]) \approx -2qk_{1B}^{\circ}[\mathrm{S}]\langle t_{BP}\rangle \tag{24}$$

indicating that sub-Poissonian behavior, as well as a linear dependence of the Poisson indicator on [S], is always expected at sufficiently low substrate concentration. This corresponds to substrate binding being so much slower than bound/intermediate state decay ($\langle\tau_1\rangle \gg \langle\tau_B\rangle$) that the latter process becomes effectively Poissonian ($\langle\tau_B^2\rangle - 2\langle\tau_B\rangle^2 \approx 0$ and $\langle\tau_B\rangle \approx \langle t_{B1}\rangle \approx \langle t_{BP}\rangle$), irrespective of the complexity of the underlying dynamics. That is, the unbinding and product formation transitions behave as rate steps with rates $k_{B1} = (1 - q)/\langle\tau_B\rangle$ and $k_{BP} = q/\langle\tau_B\rangle$, respectively, as the generic scheme reduces to the Michaelis–Menten scheme shown in Figure 3a (with $k_{1B}^{\circ}[\mathrm{S}] \ll 1/\langle\tau_B\rangle$), resulting in sub-Poissonian statistics.

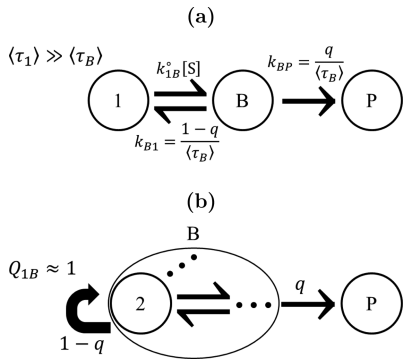

Figure 3. Reduced representations of the generic enzymatic scheme at low (a) and high (b) substrate concentration. (a) At low substrate concentration, substrate binding is much slower than bound/intermediate state decay ($\langle\tau_1\rangle \gg \langle\tau_B\rangle$), resulting in the latter process becoming effectively Poissonian, i.e., the unbinding and product formation transitions behave as rate steps, as the scheme reduces to a Michaelis–Menten model. (b) At high substrate concentration, substrate binding effectively occurs instantaneously ($Q_{1B} \approx 1$), as turnover begins in state 2 and unbinding proceeds directly back into state 2.

In the limit of high substrate concentration, the Poisson indicator approaches a constant value. Substrate binding becomes arbitrarily fast at high substrate concentrations, so the Poisson indicator will reflect the statistical properties of the steps not dependent upon substrate concentration. For the generic enzymatic reaction, the large-[S] limit is given by

$$P_{[\mathrm{S}]\to\infty} = q\frac{\langle\tau_B^2\rangle - 2\langle\tau_B\rangle\langle t_{BP}\rangle}{\langle\tau_B\rangle^2} \tag{25}$$

which is recovered when $\langle\tau_1\rangle \ll \langle\tau_B\rangle$. This corresponds to instantaneous substrate binding ($Q_{1B} \approx 1$), with turnover effectively beginning in state 2 and unbinding proceeding back into state 2, as shown in the reduced scheme in Figure 3b. We note that $P_{[\mathrm{S}]\to\infty}$ vanishes when the bound/intermediate state is unaggregated (i.e., contains a single underlying state, undergoing Poissonian decay) and can be positive when branching occurs within the bound/intermediate state. The expression for $P_{[\mathrm{S}]\to\infty}$ can be simplified with basic assumptions about the nature of the enzymatic system. Under the aforementioned perfectly evolved enzyme assumption (in which $q \approx 1$), the large-[S] limit of the Poisson indicator simplifies to

$$P_{[\mathrm{S}]\to\infty} \approx \frac{\langle t_{BP}^2\rangle - 2\langle t_{BP}\rangle^2}{\langle t_{BP}\rangle^2} \equiv P_{BP} \tag{26}$$

where we have defined P_{BP} as the Poisson indicator for product formation. Therefore, for an enzyme of this type, determination of the Poisson indicator at high substrate concentration directly informs upon the statistical properties of the step(s) converting substrate to product after substrate binding. In a similar vein, we can consider the case of an enzyme where product formation is much slower than substrate unbinding, which corresponds to the limit $q \to 0$ in our model. The large-[S] limit of the Poisson indicator is then given by

$$\begin{aligned} P_{[\mathrm{S}]\to\infty} &\approx \frac{q}{1-q}\frac{\langle t_{B1}^2\rangle - 2\langle t_{B1}\rangle\langle t_{BP}\rangle}{\langle t_{B1}\rangle^2} \\ &= \frac{q}{1-q}\left(P_{B1} + \frac{2(\langle t_{B1}\rangle - \langle t_{BP}\rangle)}{\langle t_{B1}\rangle}\right) \end{aligned} \tag{27}$$

where $P_{B1} \equiv \frac{\langle t_{B1}^2\rangle - 2\langle t_{B1}\rangle^2}{\langle t_{B1}\rangle^2}$. Hence, in this case, the large-[S] limit depends upon the Poisson indicator for the substrate unbinding process and a normalized measure of the difference in average waiting time for substrate unbinding and product formation. These limits offer another means of tying experimental measurements of the Poisson indicator to the underlying statistics, in addition to the possibility of directly fitting experimental data to the general functional form of the Poisson indicator.

We now proceed to extend our approach to more complex reaction schemes.

3.2. Competitive Inhibition. As a further example of our approach, we examine a generalized scheme for enzymatic reactions with competitive inhibition (Figure 4). We note that inhibited single-molecule reactions have experimental relevance[35] and have been the subject of theoretical studies involving rate processes.[29,36]

Now, the free enzyme may bind either substrate or inhibitor, reaching state 2 or 2* with probability p or $(1 - p)$, respectively. Like the bound/intermediate state, the inhibited state I may be an aggregate of states with an arbitrary internal topology; thus, it may undergo non-Poissonian decay. Following the same analysis as before, the overall waiting time distribution takes the form

DOI: 10.1021/acs.jpcb.7b01516
J. Phys. Chem. B XXXX, XXX, XXX–XXX

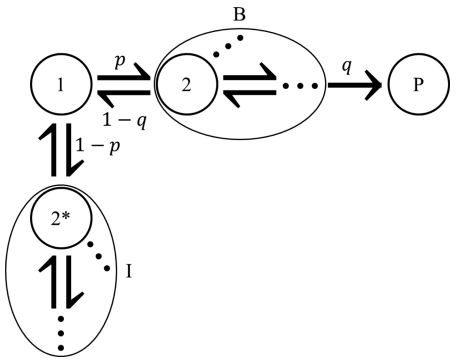

Figure 4. Generalized enzymatic reaction incorporating competitively inhibited state I, which can be an aggregate of states with an arbitrary internal topology. p and q are the branching probabilities for binding substrate (versus inhibitor) and for advancing to product from state 2, respectively.

$$\hat{\phi}(s) = \frac{Q_{1B}(s)Q_{BP}(s)}{1 - Q_{1B}(s)Q_{B1}(s) - Q_{1I}(s)Q_{I1}(s)} = \frac{\alpha}{1 - \beta} \tag{28}$$

where $Q_{1B}(s)$ and $Q_{B1}(s)$ are the waiting time distributions for substrate binding and unbinding, $Q_{1I}(s)$ and $Q_{I1}(s)$ are the distributions for inhibitor binding and unbinding, and $Q_{BP}(s)$ is the distribution for product formation. The constants α and β are then

$$\alpha = pq\left[1 - s\langle t_{1B} + t_{BP}\rangle + \frac{s^2}{2}\langle (t_{1B} + t_{BP})^2\rangle - \ldots\right] \tag{29}$$

$$\beta = p(1 - q)\left[1 - s\langle t_{1B} + t_{B1}\rangle + \frac{s^2}{2}\langle (t_{1B} + t_{B1})^2\rangle - \ldots\right] + (1 - p)\left[1 - s\langle t_{1I} + \tau_I\rangle + \frac{s^2}{2}\langle (t_{1I} + \tau_I)^2\rangle - \ldots\right] \tag{30}$$

where $\langle t_{1B}\rangle$ and $\langle t_{1B}^2\rangle$ are the first and second moments for the substrate binding waiting time, $\langle t_{1I}\rangle$ and $\langle t_{1I}^2\rangle$ are the first and second moments for the inhibitor binding waiting time, and $\langle \tau_I\rangle$ and $\langle \tau_I^2\rangle$ are the first and second moments for the decay time of the inhibited state. Again, we can examine the dependence on the concentrations of substrate and inhibitor by assuming that the binding of each is a rate process. This assumption leads to $\langle t_{1B}^k\rangle = \langle t_{1I}^k\rangle = \langle \tau_1^k\rangle$, where $\langle \tau_1^k\rangle = p\langle t_{1B}^k\rangle + (1 - p)\langle t_{1I}^k\rangle$, with

$$\langle \tau_1\rangle = \frac{1}{k_{1B} + k_{1I}} \tag{31}$$

$$p = \frac{k_{1B}}{k_{1B} + k_{1I}} \tag{32}$$

and $\langle \tau_1^2\rangle - 2\langle \tau_1\rangle^2 = 0$ for pseudo-first-order rate $k_{1I} = k_{1I}^\circ[I]$, where k_{1I}° is the rate constant for inhibitor binding, and $[I]$ is the inhibitor concentration.

The first overall waiting time moment for the enzymatic reaction in the presence of a competitive inhibitor is then

$$\langle t\rangle = \frac{1}{q}\left[\frac{1 + k_{1I}^\circ[I]\langle \tau_I\rangle}{k_{1B}^\circ[S]} + \langle \tau_B\rangle\right] \tag{33}$$

Now, calculation of the Poisson indicator as before yields

$$P([S]) = \frac{\frac{A}{[S]} + B}{\left(\frac{1}{[S]} + C\right)^2} \tag{34}$$

where A, B, and C now depend upon the inhibitor concentration and are given by

$$A = \frac{qk_{1B}^\circ}{(1 + k_{1I}^\circ[I]\langle \tau_I\rangle)^2}[-2\langle t_{BP}\rangle + k_{1I}^\circ[I](\langle \tau_I^2\rangle - 2\langle \tau_I\rangle\langle t_{BP}\rangle)] \tag{35}$$

$$B = \frac{q(k_{1B}^\circ)^2}{(1 + k_{1I}^\circ[I]\langle \tau_I\rangle)^2}[\langle \tau_B^2\rangle - 2\langle \tau_B\rangle\langle t_{BP}\rangle] \tag{36}$$

$$C = \frac{k_{1B}^\circ\langle \tau_B\rangle}{1 + k_{1I}^\circ[I]\langle \tau_I\rangle} \tag{37}$$

Notably, this is the same basic functional form (with respect to [S]) as that in the uninhibited case (eq 17). To second order, eight parameters are needed to describe the non-Poissonian kinetics (with Poissonian binding): k_{1B}°, k_{1I}°, q, $\langle \tau_B\rangle$, $\langle \tau_I\rangle$, $\langle t_{BP}\rangle$, $\langle \tau_B^2\rangle$, and $\langle \tau_I^2\rangle$. However, eqs 33−37 indicate that fitting (with respect to [S] and [I]) to second order only gives six independent parameters, making the kinetics underdetermined by two parameters. However, the number of underdetermined parameters can be reduced in several situations. (i) If either k_{1B}° or k_{1I}° is known, then one kinetic parameter can be eliminated (two if both are known). (ii) If inhibitor unbinding is a rate process with rate k_{1I}, then $\langle \tau_I\rangle = 1/k_{1I}$ and $\langle \tau_I^2\rangle - 2\langle \tau_I\rangle^2 = 0$, which eliminates one kinetic parameter. (iii) If the aforementioned perfectly evolved enzyme assumption holds, then the number of underdetermined parameters is reduced by one (as shown in section 3.1.1). (iv) If the bound/intermediate state undergoes Poissonian decay, then the number of underdetermined parameters is also reduced by one (as shown in section 3.1.1). Thus, the kinetics can be specified in a variety of ways.

Figure 5a illustrates the dependence of the Poisson indicator on substrate concentration across a range of inhibitor concentrations. As was the case for the uninhibited reaction, the Poisson indicator vanishes at very low substrate concentration and adopts the form given in eq 25 at high substrate concentration. The large-[S] limits match for these two cases because, from eqs 31 and 32, when $k_{1B}^\circ[S] \gg k_{1I}^\circ[I]$, $\langle \tau_1\rangle \approx \frac{1}{k_{1B}^\circ[S]}$ and $p \approx 1$. Qualitative differences are evident between Figures 2 and 5a. In particular, a local maximum (with respect to [S]) can be achieved with a competitive inhibitor when $AC > B$ and $C > 2B/A$. This unique feature corresponds to the point of maximal dispersion for a given, obtainable A, B, and C (capable of achieving one). We note that $P([S])$ may instead achieve a local minimum or no realizable local extremum. In the presence of a competitive inhibitor, eq 24 for low [S] does not generally apply (except in the limit of vanishing [I]). In fact, under certain conditions, the Poisson indicator can be non-negative at all substrate concentrations, precluding sub-Poissonian behavior. Similarly, the Poisson indicator can be nonpositive at all substrate concentrations under certain conditions (behavior not shown in Figure 5a), even when a competitive inhibitor is present.

The inherent asymmetry between inhibitor and substrate is demonstrated in Figure 5b, where the Poisson indicator is

DOI: 10.1021/acs.jpcb.7b01516
J. Phys. Chem. B XXXX, XXX, XXX−XXX

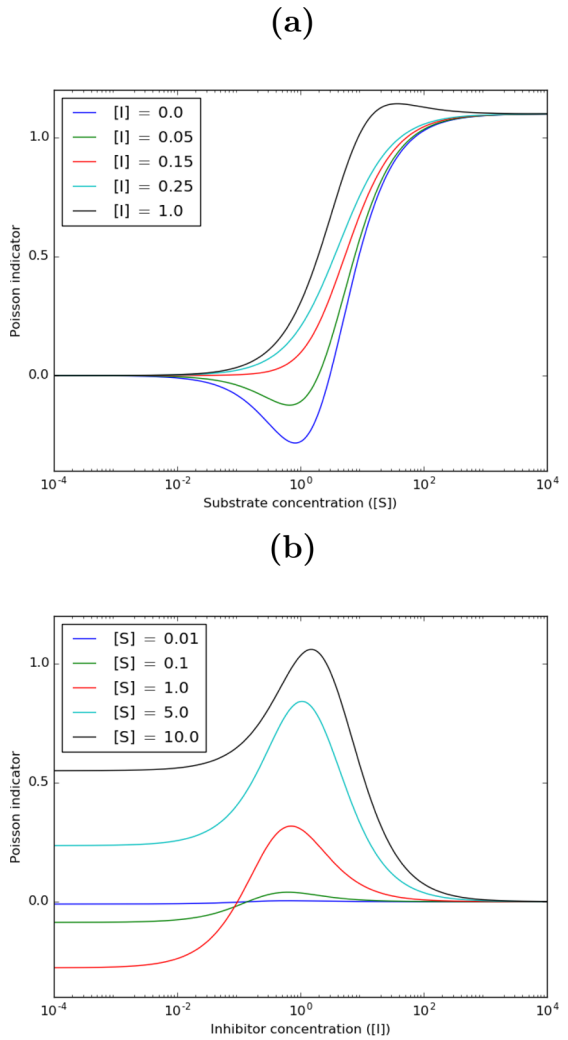

Figure 5. (a) Plot of the Poisson indicator versus substrate concentration at fixed inhibitor concentration. The numerical parameters are $k^{\circ}_{IB} = 1$, $k^{\circ}_{II} = 1$, $q = 0.5$, $\langle\tau_B\rangle = 0.55$, $\langle\tau_I\rangle = 3$, $\langle t_{BP}\rangle = 1$, $\langle\tau_B^2\rangle = 1.765$, and $\langle\tau_I^2\rangle = 20$, with [I] given in the legend. (b) Plot of the Poisson indicator versus inhibitor concentration at fixed substrate concentration. The numerical parameters are identical to those in (a), except now [S] is given in the legend.

plotted against inhibitor concentration across a range of substrate concentrations. The Poisson indicator can attain a local maximum (with respect to [I]), which corresponds to the point of maximal dispersion for a given set of conditions (under which one can be achieved). We note that $P([I])$ may instead achieve a local minimum or no realizable local extremum (cases not shown in Figure 5b). In the limit of saturating [I], P vanishes because inhibitor binding becomes the only feasible transition. As is to be expected, eqs 35−37 above reduce to the results for the generic enzymatic reaction in the limit of vanishing [I].

3.3. Multiple Substrates. Our methodology can also be applied to more complex systems. In fact, generalization to a reaction with multiple substrates is straightforward. The scheme for this case is illustrated in Figure 6. The waiting time distribution for the conversion of any one of the n substrates to its corresponding product is given by

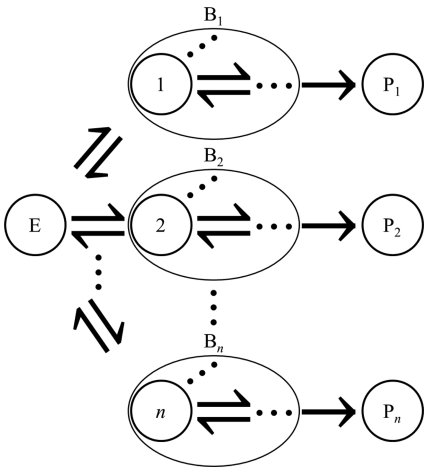

Figure 6. Generalized enzymatic reaction featuring n competing substrates with concentrations $[S_1]$, $[S_2]$, ..., $[S_n]$.

$$\hat{\phi}(s) = \frac{\sum_i Q_{EB_i}(s) Q_{B_iP}(s)}{1 - \sum_i Q_{EB_i}(s) Q_{B_iE}(s)} = \frac{\alpha}{1 - \beta} \tag{38}$$

where $Q_{EB_i}(s)$ is the waiting time distribution for the binding of substrate S_i, $Q_{B_iE}(s)$ is the distribution for the unbinding of substrate S_i, and $Q_{B_iP}(s)$ is the distribution for the conversion of bound/intermediate state B_i to the corresponding product P_i. In terms of the waiting time moments for the individual steps,

$$\alpha = \sum_i p_i q_i \left[1 - s\langle t_{EB_i} + t_{B_iP}\rangle + \frac{s^2}{2}\langle (t_{EB_i} + t_{B_iP})^2\rangle\right] \tag{39}$$

$$\beta = \sum_i p_i (1 - q_i) \left[1 - s\langle t_{EB_i} + t_{B_iE}\rangle + \frac{s^2}{2}\langle (t_{EB_i} + t_{B_iE})^2\rangle\right] \tag{40}$$

where q_i is the branching probability for the formation of product P_i, $\langle t_{EB_i}\rangle$ and $\langle t_{EB_i}^2\rangle$ are the first and second waiting time moments for the binding of substrate S_i, $\langle t_{B_iE}\rangle$ and $\langle t_{B_iE}^2\rangle$ are the first and second waiting time moments for the unbinding of substrate S_i, and $\langle t_{B_iP}\rangle$ and $\langle t_{B_iP}^2\rangle$ are the first and second moments for the formation of product P_i. Assuming that the binding of any substrate is a rate process, then $\langle t_{EB_i}\rangle = \langle\tau_E\rangle$ and $\langle t_{EB_i}^2\rangle = \langle\tau_E^2\rangle$, where $\langle\tau_E\rangle = \sum_i p_i \langle t_{EB_i}\rangle$ and $\langle\tau_E^2\rangle = \sum_i p_i \langle t_{EB_i}^2\rangle$ are the first and second waiting time moments, respectively, for the decay of the initial free enzyme state, with p_i representing the probability of binding substrate S_i. We now have p_i and $\langle\tau_E\rangle$ given by

$$p_i = \frac{k_{EB_i}}{\sum_i k_{EB_i}} \tag{41}$$

$$\langle\tau_E\rangle = \frac{1}{\sum_i k_{EB_i}} \tag{42}$$

as well as $\langle\tau_E^2\rangle - 2\langle\tau_E\rangle^2 = 0$, with pseudo-first-order rate $k_{EB_i} = k^{\circ}_{EB_i}[S_i]$, where $k^{\circ}_{EB_i}$ is the rate constant for the binding of substrate S_i.

The first moment for the overall waiting time in the presence of multiple substrates is expressed as

DOI: 10.1021/acs.jpcb.7b01516
J. Phys. Chem. B XXXX, XXX, XXX−XXX

$$\langle t \rangle = \frac{1 + \sum_i k^\circ_{\mathrm{EB}_i}[\mathrm{S}_i]\langle \tau_{\mathrm{B}_i}\rangle}{\sum_i q_i k^\circ_{\mathrm{EB}_i}[\mathrm{S}_i]} \tag{43}$$

where $\langle \tau_{\mathrm{B}_i}\rangle = q_i\langle t_{\mathrm{B}_i\mathrm{P}}\rangle + (1 - q_i)\langle t_{\mathrm{B}_i\mathrm{E}}\rangle$ is the first waiting time moment for the decay of bound/intermediate state B_i. Now, if we choose to examine the dependence of the Poisson indicator on the concentration of a single substrate $[\mathrm{S}_k]$, it will have the following functional form:

$$P([\mathrm{S}_k]) = \frac{\frac{A}{[\mathrm{S}_k]^2} + \frac{B}{[\mathrm{S}_k]} + C}{\left(\frac{1}{[\mathrm{S}_k]} + D\right)^2} \tag{44}$$

which notably departs from the functional form presented above for the single-substrate and competitively inhibited cases (eq 17). The constants A, B, C, and D, all independent of $[\mathrm{S}_k]$, have expressions

$$A = \zeta^2[-2\sum_{i\neq k} q_i k^\circ_{\mathrm{EB}_i}[\mathrm{S}_i]\langle t_{\mathrm{B}_i\mathrm{P}}\rangle + \sum_{i\neq k, j\neq k} k^\circ_{\mathrm{EB}_i}[\mathrm{S}_i] q_j k^\circ_{\mathrm{EB}_j}[\mathrm{S}_j] (\langle \tau^2_{\mathrm{B}_i}\rangle - 2\langle \tau_{\mathrm{B}_i}\rangle\langle t_{\mathrm{B}_j\mathrm{P}}\rangle)] \tag{45}$$

$$B = \zeta^2[-2q_k k^\circ_{\mathrm{EB}_k}\langle t_{\mathrm{B}_k\mathrm{P}}\rangle + \sum_{i\neq k} q_i k^\circ_{\mathrm{EB}_k} k^\circ_{\mathrm{EB}_i}[\mathrm{S}_i] (\langle \tau^2_{\mathrm{B}_k}\rangle - 2\langle \tau_{\mathrm{B}_k}\rangle\langle t_{\mathrm{B}_i\mathrm{P}}\rangle) + \sum_{i\neq k} q_k k^\circ_{\mathrm{EB}_k} k^\circ_{\mathrm{EB}_i}[\mathrm{S}_i] (\langle \tau^2_{\mathrm{B}_i}\rangle - 2\langle \tau_{\mathrm{B}_i}\rangle\langle t_{\mathrm{B}_k\mathrm{P}}\rangle)] \tag{46}$$

$$C = \zeta^2 q_k (k^\circ_{\mathrm{EB}_k})^2 (\langle \tau^2_{\mathrm{B}_k}\rangle - 2\langle \tau_{\mathrm{B}_k}\rangle\langle t_{\mathrm{B}_k\mathrm{P}}\rangle) \tag{47}$$

$$D = \zeta k^\circ_{\mathrm{EB}_k}\langle \tau_{\mathrm{B}_k}\rangle \tag{48}$$

where $\langle \tau^2_{\mathrm{B}_i}\rangle = q_i\langle t^2_{\mathrm{B}_i\mathrm{P}}\rangle + (1 - q_i)\langle t^2_{\mathrm{B}_i\mathrm{E}}\rangle$ is the second waiting time moment for the decay of bound/intermediate state B_i, and we have defined

$$\zeta = \frac{1}{1 + \sum_{i\neq k} k^\circ_{\mathrm{EB}_i}[\mathrm{S}_i]\langle \tau_{\mathrm{B}_i}\rangle} \tag{49}$$

As a simple example of the behavior of the Poisson indicator in the presence of multiple substrates, the Poisson indicator is calculated for two competing substrates S_a and S_b. In Figure 7, the Poisson indicator is plotted against the concentration of S_a at a fixed concentration of S_b. We note that in this plot, $\langle t^2_{\mathrm{B}_b\mathrm{E}}\rangle$ and $\langle t^2_{\mathrm{B}_b\mathrm{P}}\rangle$ are held fixed while q_b is varied, causing $\langle \tau^2_{\mathrm{B}_b}\rangle$ to also vary, but q_b could instead be varied while holding $\langle \tau^2_{\mathrm{B}_b}\rangle$ fixed.

For $[\mathrm{S}_a] = 0$, the single-substrate result at fixed $[\mathrm{S}_b]$ is obtained as $P([\mathrm{S}_a] = 0) = A$, which can be nonzero, differing from $P([\mathrm{S}] = 0)$ for the above two cases. In the limit of saturating $[\mathrm{S}_a]$, the single-substrate form for $P_{[\mathrm{S}_a]\to\infty}$ (eq 25) is obtained. It should be noted that earlier results are recovered in the appropriate limits: setting $[\mathrm{S}_{i\neq k}] = 0$ recovers the single-substrate expression for $P([\mathrm{S}_k])$ (eq 16). In addition, for only two competing substrates S_a and S_b, as in Figure 7, setting the branching probability $q_b = 0$ recovers the competitive inhibition result for $P([\mathrm{S}_a])$ (eqs 34−37), where $[\mathrm{S}_b]$ corresponds to the inhibitor concentration. In fact, $P([\mathrm{S}_a])$ can achieve a local maximum similar to that shown in Figure 5a for competitive inhibition. We identify the presence of such a maximum for a renewal process as a signature of competitive binding, either between a substrate and an inhibitor or between multiple substrates. Finally, if the substrates are taken to be identical, that is $[\mathrm{S}] = [\mathrm{S}_1] = [\mathrm{S}_2] = \ldots = [\mathrm{S}_n]$, then eq 44 describes the Poisson indicator for an enzymatic reaction of a single substrate with multiple, parallel pathways, nearly analogous to earlier results for ion channel statistics.[20]

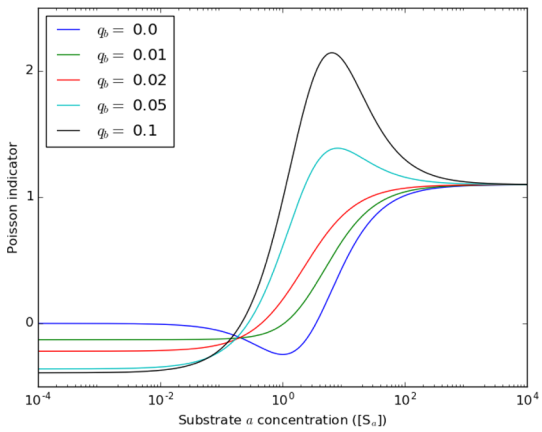

Figure 7. Plot of the Poisson indicator versus $[\mathrm{S}_a]$ for two competing substrates S_a and S_b. The numerical parameters are $k^\circ_{\mathrm{EB}_a} = 1$, $k^\circ_{\mathrm{EB}_b} = 1$, $q_a = 0.5$, $[\mathrm{S}_b] = 1$, $\langle \tau_{\mathrm{B}_a}\rangle = 0.55$, $\langle t_{\mathrm{B}_a\mathrm{P}}\rangle = 1$, $\langle t_{\mathrm{B}_b\mathrm{E}}\rangle = 0.3$, $\langle t_{\mathrm{B}_b\mathrm{P}}\rangle = 10$, $\langle \tau^2_{\mathrm{B}_a}\rangle = 1.765$, $\langle t^2_{\mathrm{B}_b\mathrm{E}}\rangle = 0.25$, and $\langle t^2_{\mathrm{B}_b\mathrm{P}}\rangle = 250$, with q_b given in the legend. Note that the case of $q_b = 0$ is equivalent to substrate S_a competing with inhibitor S_b.

4. CONCLUSIONS

A general methodology for calculating second moments for the waiting time between reaction events has been introduced and applied to the analysis of enzymatic reactions. All of the flexibility conferred by the self-consistent pathway analysis method (paper 1)[15] is retained, and the approach can be applied to many diverse cases. Our approach is currently restricted to renewal processes but will be extended to nonrenewal processes in a subsequent paper (paper 3). In the current study, the principal results concern a generic enzymatic reaction as well as the more complex cases of competitive inhibition and multiple substrates, without assuming all states undergo Poissonian decay. The use of a generic model of enzyme catalysis allows the determination of the maximum information content of measurements of the Poisson indicator and first waiting time moment. Furthermore, analytical expressions for the Poisson indicator as a function of substrate concentration allow connections to be made between experimental data and kinetic models.

Our specific findings are summarized as follows: (i) based upon fitting to the functional forms of the first two waiting time moments, the non-Poissonian kinetics are generally underdetermined to second order but can be specified under certain circumstances. (ii) For a generic enzymatic scheme with an arbitrary intermediate topology, sub-Poissonian statistics can always (for nontrivial kinetics) be achieved for a certain range of substrate concentrations, even when branching occurs out of the intermediate state(s). (iii) We have identified a generic minimum of the Poisson indicator (with respect to substrate concentration), and this can be used to tune substrate concentration to the stochastic fluctuations, attaining minimal turnover event dispersion, and to estimate the largest number

DOI: 10.1021/acs.jpcb.7b01516
J. Phys. Chem. B XXXX, XXX, XXX−XXX

of underlying consecutive rate steps in a turnover cycle (demonstrative example provided in Appendix A). (iv) At high and low substrate concentration, the Poisson indicator reflects the effective reduction of the generic enzymatic scheme based upon the rate-determining process. (v) We have identified a local maximum of the Poisson indicator as a function of substrate concentration for a renewal process as a signature of competitive binding, either between a substrate and an inhibitor or between multiple substrates. Our analysis may be easily extended to other single-molecule experiments, offering the same benefits. In particular, application to the study of motor proteins may be fruitful due to the presence of reaction steps dependent upon substrate concentration as well as the applied mechanical force.[37]

APPENDIX A

Here, we provide a demonstrative example of how the functional forms of the mean first-passage time and Poisson indicator for the generic enzymatic reaction scheme in Figure 1 (shown in eqs 14 and 17, respectively) can be used to reveal experimentally accessible information about the underlying scheme. Consider the underlying reaction scheme illustrated in Figure 8, which consists of a three-link chain. In a single-enzyme experiment, the intermediate topology, i.e., what occurs between substrate binding and the final transition to product, is presumably not known. Thus, we aim to show the information about this intermediate topology that can be obtained from measurements of the first two waiting time moments and [S].

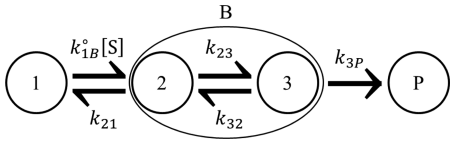

Figure 8. Example of an underlying enzymatic reaction scheme corresponding to the generic model in Figure 1. The values of the underlying rate constants are $k^{\circ}_{1B} = 1$, $k_{21} = 0.5$, $k_{23} = 2$, $k_{32} = 0.6$, and $k_{3P} = 3$.

In order to obtain the four independent, experimentally accessible parameters in eqs 14 and 17, $[qk^{\circ}_{1B}]^{-1}$, $\langle\tau_B\rangle/q$, A, and B, we first evaluate the non-Poissonian kinetic parameters q, $\langle t_{BP}\rangle$, $\langle\tau_B\rangle$, and $\langle\tau_B^2\rangle$ from the underlying rates shown in Figure 8. As indicated in section 3.1.1, these non-Poissonian kinetic parameters cannot generally all be obtained from experiments (although they can be in certain scenarios, one of which we address below); thus, we evaluate them here as a means of obtaining the aforementioned experimentally accessible parameters. For this scheme, $Q_{B1}(s)$ and $Q_{BP}(s)$ are expressed in terms of the waiting time distributions for the underlying transitions as

$$Q_{B1}(s) = \frac{Q_{21}(s)}{1 - Q_{23}(s)Q_{32}(s)} \tag{50}$$

$$Q_{BP}(s) = \frac{Q_{23}(s)Q_{3P}(s)}{1 - Q_{23}(s)Q_{32}(s)} \tag{51}$$

The waiting time distributions for the underlying transitions are expanded in terms of their moments according to eq 5, and since each underlying transition is a rate process, $q_{ij} = k_{ij}/(\sum_j k_{ij})$ and $\langle t_{ij}^n\rangle = n!q_{ij}^n/k_{ij}^n$. The product formation branching probability $q = Q_{BP}(s = 0)$ is thus expressed in terms of the underlying rates as

$$q = \frac{k_{23}k_{3P}}{k_{21}(k_{32} + k_{3P}) + k_{23}k_{3P}} \tag{52}$$

The distribution $Q_{BP}(s)$ is differentiated to obtain $\langle t_{BP}\rangle = -q^{-1}\mathrm{d}Q_{BP}(s)/\mathrm{d}s|_{s=0}$ as

$$\langle t_{BP}\rangle = \frac{k_{21} + k_{23} + k_{32} + k_{3P}}{k_{21}(k_{32} + k_{3P}) + k_{23}k_{3P}} \tag{53}$$

Similarly, the B decay time distribution, $[Q_{B1}(s) + Q_{BP}(s)]$, is differentiated to obtain $\langle\tau_B\rangle = -\mathrm{d}/\mathrm{d}s[Q_{B1}(s) + Q_{BP}(s)]|_{s=0}$ and $\langle\tau_B^2\rangle = \mathrm{d}^2/\mathrm{d}s^2[Q_{B1}(s) + Q_{BP}(s)]|_{s=0}$ as

$$\langle\tau_B\rangle = \frac{k_{23} + k_{32} + k_{3P}}{k_{21}(k_{32} + k_{3P}) + k_{23}k_{3P}} \tag{54}$$

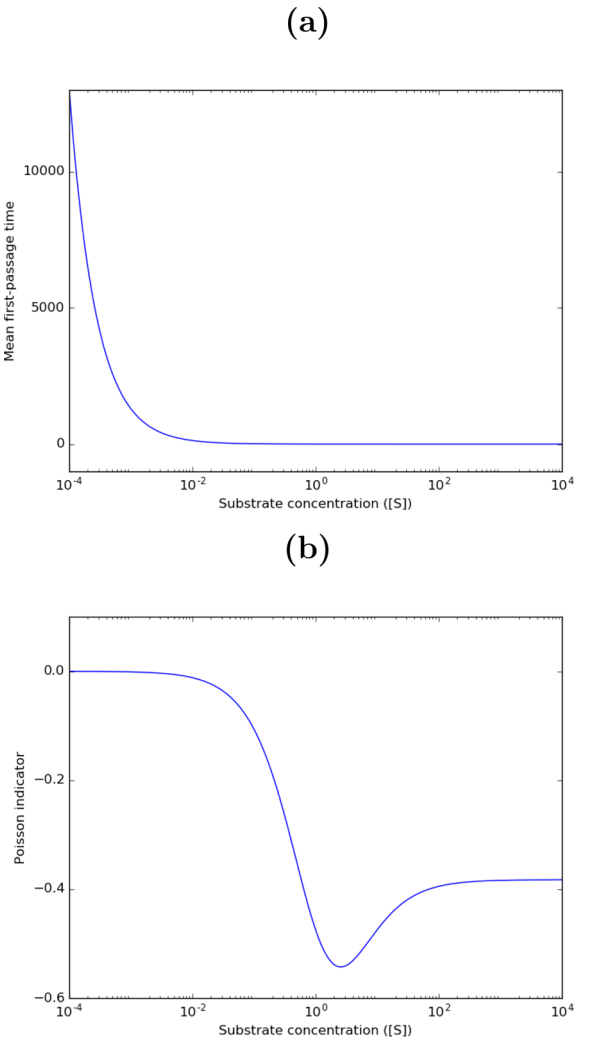

Figure 9. Plots of the (a) mean first-passage time and (b) Poisson indicator versus substrate concentration for the underlying enzymatic reaction scheme shown in Figure 8. The values of the four independent, experimentally accessible parameters from the general functional forms of the mean first-passage time and Poisson indicator (shown in eqs 14 and 17, respectively) are $[qk^{\circ}_{1B}]^{-1} = 1.3$, $\langle\tau_B\rangle/q = 0.933$, $A = -1.20$, and $B = -0.197$.

DOI: 10.1021/acs.jpcb.7b01516
J. Phys. Chem. B XXXX, XXX, XXX−XXX

$$\langle \tau_B^2 \rangle = 2\frac{(k_{23} + k_{32} + k_{3P})^2 + k_{23}(k_{21} - k_{3P})}{[k_{21}(k_{32} + k_{3P}) + k_{23}k_{3P}]^2} \quad (55)$$

For the values of the underlying rates given in Figure 8, $q = 10/13$, $\langle t_{BP} \rangle = 61/78$, $\langle \tau_B \rangle = 28/39$, and $\langle \tau_B^2 \rangle = 1318/1521$. Thus, $[qk_{1B}^\circ]^{-1} = 1.3$, $\langle \tau_B \rangle / q = 0.933$, $A = -1.20$, and $B = -0.197$, with $C = (\langle \tau_B \rangle / q)/[qk_{1B}^\circ]^{-1} = 0.718$. Now, the mean first-passage time and Poisson indicator are evaluated as functions of [S] from eqs 14 and 17−20 and plotted in Figure 9, with these plots resembling what could be obtained in a single-enzyme experiment.

From the mean first-passage time and Poisson indicator as functions of [S], we can now use the generic minimum of $P([S])$ to estimate the number of consecutive links in the underlying turnover cycle. We note that because the underlying scheme is unicyclic, $M_{max} = M$, although this would not necessarily be known in an experiment. Since $AC < 2B$ here (i.e., $\langle \tau_B^2 \rangle > \langle \tau_B \rangle \langle t_{BP} \rangle$), $P([S])$ is minimized at [S]*, so the inequality for M in eq 22 is applicable. From this inequality, the lower bound on M is $[1 + A^2/(4[AC - B])]^{-1} = 2.2$. Since this is not a whole number, and since the underlying scheme cannot be a homogeneous, sequential chain (which would minimize P with respect to the entire set of underlying rates) due to q being less than unity, the underlying cycle must contain at least three rate steps. Therefore, from the experimentally accessible information, M is estimated to be 3, which—as we know from Figure 8—is the correct number of underlying links. Thus, in this case, the underlying reaction scheme can be completely inferred from measurements of the first two waiting time moments and [S]. In addition, if k_{1B}° is known or can be estimated, then q, $\langle t_{BP} \rangle$, $\langle \tau_B \rangle$, and $\langle \tau_B^2 \rangle$ can all be determined from the experimentally accessible parameters, permitting complete specification of the non-Poissonian kinetics (with Poissonian binding) and, in this case, determination of all underlying rates (since there are exactly four besides that for substrate binding).

AUTHOR INFORMATION

Corresponding Author

*E-mail: jianshu@mit.edu.

ORCID

D. Evan Piephoff: 0000-0002-8556-7414

Author Contributions

‡T.R.A. and D.E.P. contributed equally to this work.

Notes

The authors declare no competing financial interest.

ACKNOWLEDGMENTS

This work was supported by the Singapore-MIT Alliance for Research and Technology (SMART) and the NSF (Grant No. CHE-1112825). D.E.P. acknowledges support from the NSF Graduate Research Fellowship Program.

REFERENCES

(1) Park, H.; Toprak, E.; Selvin, P. R. Single-molecule fluorescence to study molecular motors. *Q. Rev. Biophys.* **2007**, *40*, 87.

(2) Chen, Y.; Hu, D.; Vorpagel, E. R.; Lu, H. P. Probing Single-Molecule T4 Lysozyme Conformational Dynamics by Intramolecular Fluorescence Energy Transfer. *J. Phys. Chem. B* **2003**, *107*, 7947−7956.

(3) Deindl, S.; Zhuang, X. Monitoring Conformational Dynamics with Single-Molecule Fluorescence Energy Transfer: Applications in Nucleosome Remodeling. *Methods Enzymol.* **2012**, *513*, 59−86.

(4) Shen, H.; Zhou, X.; Zou, N.; Chen, P. Single-Molecule Kinetics Reveals a Hidden Surface Reaction Intermediate in Single-Nanoparticle Catalysis. *J. Phys. Chem. C* **2014**, *118*, 26902−26911.

(5) Pressé, S.; Lee, J.; Dill, K. A. Extracting Conformational Memory from Single-Molecule Kinetic Data. *J. Phys. Chem. B* **2013**, *117*, 495−502.

(6) Cao, J. Event-averaged measurements of single-molecule kinetics. *Chem. Phys. Lett.* **2000**, *327*, 38−44.

(7) Flomenbom, O.; Silbey, R. J. Utilizing the information content in two-state trajectories. *Proc. Natl. Acad. Sci. U. S. A.* **2006**, *103*, 10907−10910.

(8) Qian, H.; Elson, E. L. Single-molecule enzymology: stochastic Michaelis−Menten kinetics. *Biophys. Chem.* **2002**, *101−102*, 565−576.

(9) Bruno, W. J.; Yang, J.; Pearson, J. E. Using independent open-to-closed transitions to simplify aggregated Markov models of ion channel gating kinetics. *Proc. Natl. Acad. Sci. U. S. A.* **2005**, *102*, 6326−6331.

(10) Flomenbom, O.; Klafter, J.; Szabo, A. What Can One Learn from Two-State Single-Molecule Trajectories? *Biophys. J.* **2005**, *88*, 3780−3783.

(11) Gopich, I. V.; Szabo, A. Theory of the statistics of kinetic transitions with application to single-molecule enzyme catalysis. *J. Chem. Phys.* **2006**, *124*, 154712.

(12) Ge, H. Waiting Cycle Times and Generalized Haldane Equality in the Steady-State Cycle Kinetics of Single Enzymes. *J. Phys. Chem. B* **2008**, *112*, 61−70.

(13) Kolomeisky, A. B. Michaelis−Menten relations for complex enzymatic networks. *J. Chem. Phys.* **2011**, *134*, 155101.

(14) Ochoa, M. A.; Zhou, X.; Chen, P.; Loring, R. F. Interpreting single turnover catalysis measurements with constrained mean dwell times. *J. Chem. Phys.* **2011**, *135*, 174509.

(15) Cao, J.; Silbey, R. J. Generic Schemes for Single-Molecule Kinetics. 1: Self-Consistent Pathway Solutions for Renewal Processes. *J. Phys. Chem. B* **2008**, *112*, 12867−12880.

(16) English, B. P.; Min, W.; van Oijen, A. M.; Lee, K. T.; Luo, G.; Sun, H.; Cherayil, B. J.; Kou, S. C.; Xie, X. S. Ever-fluctuating single enzyme molecules: Michaelis-Menten equation revisited. *Nat. Chem. Biol.* **2006**, *2*, 87−94.

(17) Kou, S. C.; Cherayil, B. J.; Min, W.; English, B. P.; Xie, X. S. Single-Molecule Michaelis−Menten Equations. *J. Phys. Chem. B* **2005**, *109*, 19068−19081.

(18) Jung, W.; Yang, S.; Sung, J. Novel Chemical Kinetics for a Single Enzyme Reaction: Relationship between Substrate Concentration and the Second Moment of Enzyme Reaction Time. *J. Phys. Chem. B* **2010**, *114*, 9840−9847.

(19) Yang, S.; Cao, J.; Silbey, R. J.; Sung, J. Quantitative Interpretation of the Randomness in Single Enzyme Turnover Times. *Biophys. J.* **2011**, *101*, 519−524.

(20) Chaudhury, S.; Cao, J.; Sinitsyn, N. A. Universality of Poisson Indicator and Fano Factor of Transport Event Statistics in Ion Channels and Enzyme Kinetics. *J. Phys. Chem. B* **2013**, *117*, 503−509.

(21) Kumar, A.; Maity, H.; Dua, A. Parallel versus Off-Pathway Michaelis−Menten Mechanism for Single-Enzyme Kinetics of a Fluctuating Enzyme. *J. Phys. Chem. B* **2015**, *119*, 8490−8500.

(22) Barkai, E.; Jung, Y.; Silbey, R. Theory of Single-Molecule Spectroscopy: Beyond the Ensemble Average. *Annu. Rev. Phys. Chem.* **2004**, *55*, 457−507.

(23) Mandel, L. Sub-Poissonian photon statistics in resonance fluorescence. *Opt. Lett.* **1979**, *4*, 205.

(24) Svoboda, K.; Mitra, P. P.; Block, S. M. Fluctuation analysis of motor protein movement and single enzyme kinetics. *Proc. Natl. Acad. Sci. U. S. A.* **1994**, *91*, 11782−11786.

(25) Daniels, B.; Mugler, A.; Sinitsyn, N.; Nemenman, I.; de Ronde, W. Mesoscopic statistical properties of multistep enzyme-mediated reactions. *IET Syst. Biol.* **2009**, *3*, 429−437.

(26) Takagi, H.; Nishikawa, M. Mechanochemical Coupling Revealed by the Fluctuation Analysis of Different Biomolecular Motors. *Adv. Chem. Phys.* **2011**, *146*, 419−435.

(27) Cox, D. R. *Renewal Theory*; Methuen: London, U.K., 1962.

DOI: 10.1021/acs.jpcb.7b01516
J. Phys. Chem. B XXXX, XXX, XXX−XXX

(28) Moffitt, J. R.; Bustamante, C. Extracting signal from noise: kinetic mechanisms from a Michaelis−Menten-like expression for enzymatic fluctuations. *FEBS J.* **2014**, *281*, 498−517.
(29) Chaudhury, S. Poisson Indicator and Fano Factor for Probing Dynamic Disorder in Single-Molecule Enzyme Inhibition Kinetics. *J. Phys. Chem. B* **2014**, *118*, 10405−10412.
(30) Wierenga, R. K.; Kapetaniou, E. G.; Venkatesan, R. Triosephosphate isomerase: a highly evolved biocatalyst. *Cell. Mol. Life Sci.* **2010**, *67*, 3961−3982.
(31) Cao, J. Michaelis−Menten Equation and Detailed Balance in Enzymatic Networks. *J. Phys. Chem. B* **2011**, *115*, 5493−5498.
(32) Wu, J.; Cao, J. Generalized Michaelis−Menten Equation for Conformation-Modulated Monomeric Enzymes. *Adv. Chem. Phys.* **2011**, *146*, 329−365.
(33) Piephoff, D. E.; Wu, J.; Cao, J. Conformational Nonequilibrium Enzyme Kinetics: Generalized Michaelis−Menten Equation. *J. Phys. Chem. Lett.* **2017**, *8*, 3619−3623.
(34) Barato, A. C.; Seifert, U. Universal Bound on the Fano Factor in Enzyme Kinetics. *J. Phys. Chem. B* **2015**, *119*, 6555−6561.
(35) Piwonski, H. M.; Goomanovsky, M.; Bensimon, D.; Horovitz, A.; Haran, G. Allosteric inhibition of individual enzyme molecules trapped in lipid vesicles. *Proc. Natl. Acad. Sci. U. S. A.* **2012**, *109*, E1437−E1443.
(36) Saha, S.; Sinha, A.; Dua, A. Single-molecule enzyme kinetics in the presence of inhibitors. *J. Chem. Phys.* **2012**, *137*, 045102.
(37) Keller, D.; Bustamante, C. The Mechanochemistry of Molecular Motors. *Biophys. J.* **2000**, *78*, 541−556.

DOI: 10.1021/acs.jpcb.7b01516
J. Phys. Chem. B XXXX, XXX, XXX−XXX